The Pulmonary Vascular Lesions of the Adult Respiratory Distress Syndrome

JOSEPH F. TOMASHEFSKI, Jr., MD, PAUL DAVIES, PhD, CAROLINE BOGGIS, MD, REGINALD GREENE, MD, WARREN M. ZAPOL, MD, and LYNNE M. REID, MD

From the Department of Pathology, Children's Hospital Medical Center, and the Departments of Anesthesia and Radiology, Massachusetts General Hospital, Boston, Massachusetts

Specimen arteriography, morphometry, and light and electron microscopy were used for examination of the pulmonary vasculature of 22 patients who died with the adult respiratory distress syndrome (ARDS), for the purpose of defining the lesions that contribute to pulmonary hypertension in this setting. The different lesions correlated with the duration rather than the cause of ARDS. Thromboemboli occurred in 21 patients, and macrothrombi found at autopsy correlated with the number of filling defects on antemortem angiography. Acute endothelial injury was documented ultrastructurally even in intermediate and late-stage patients. Fibrocellular intimal obliteration of arteries, veins, and lymphatics and infective vasculitis were prominent in those surviving beyond 10 days. In long-term survivors, tortuous arteries and irregularly dilated capillaries were striking features. Peripheral extension of vascular smooth muscle and a significant increase in the percentage of medial thickness of muscular arteries with duration of ARDS were noted. The pathogenesis and clinical significance of these lesions is discussed. (Am J Pathol 1983, 112:112–126)

PULMONARY vascular injury is a central feature of the adult respiratory distress syndrome (ARDS), and pulmonary hypertension due to an increased pulmonary vascular resistance is virtually always present.[1] Recent advances in mechanical ventilation and intensive care of the critically ill have extended the life span of patients with severe acute respiratory failure to several weeks' duration.[2] Early in ARDS pulmonary vasoconstriction, thromboembolism, and interstitial edema, features that are potentially reversible, can raise the pulmonary artery pressure, but after several weeks more serious structural changes such as obliteration of the microcirculation and increased arterial muscularization also contribute to pulmonary hypertension.[3–8] Pulmonary vascular obliteration and muscularization were recently analyzed morphometrically in an autopsy series of 11 ARDS patients.[7] Otherwise, little quantitative information is available on the range of pathologic alterations in arteries, veins, and lymphatics found in patients dying from ARDS of varying duration. The chronic arterial changes, particularly, have received little emphasis.

The present report describes an analysis of the pulmonary vascular findings in 22 patients (including 11 described by Snow et al[7]), using postmortem arteriography, vascular morphometry, and light and electron microscopy. It extends that report to describe fully the histologic features and postmortem arteriographic appearance of all of the vascular lesions and correlates these in each patient with clinical and laboratory measurements, the course of the acute lung disease, and its cause.

Supported by NHLBI SCOR Grant 23591 and in part by Grant RR-01032 from the General Clinical Research Centers Program of the Division of Research Resources, National Institutes of Health. Data organization and analysis was performed on the PROPHET system, a national computer resource sponsored by the Division of Research Resources, National Institutes of Health.

Presented at the American Thoracic Society meeting in Los Angeles, California, May 16, 1982.

Accepted for publication March 4, 1983.

Address reprint requests to Lynne M. Reid, MD, Department of Pathology, Children's Hospital Medical Center, 300 Longwood Avenue, Boston MA 02115.

Address correspondence to Joseph F. Tomashefski, Jr., MD, Department of Pathology, Cleveland Metropolitan General Hospital, 3395 Scranton Road, Cleveland, OH 44109.

0002-9440/83/0707-0112$01.55

Materials and Methods

Patient Data

In this series there were 22 patients, 11 men and 11 women, ranging in age from 16 to 76 years (median, 31 years). The initial causes of ARDS were sepsis (5 patients), trauma (4), virus or mycoplasma pneumonia (6), aspiration of stomach contents (4), bacterial pneumonia (2), and toxic inhalation (1). ARDS was diagnosed by the sudden onset of dyspnea with bilateral diffuse infiltrates in the chest radiograph and hypoxemia (Pa_{O_2} <50 mm Hg at an FI_{O_2} of 0.5). All patients had an endotracheal tube in place and were treated with supplemental oxygen (FI_{O_2} >0.5) and mechanically ventilated with positive end expiratory pressure between 5 and 20 cm H_2O in the respiratory intensive care unit of the Massachusetts General Hospital. The mean pulmonary artery pressure ($\overline{PAP}$) was measured at end expiration with a Swan-Ganz catheter using a Statham P27DB transducer and a Hewlett Packard recorder. Zero pressure was taken as atmospheric pressure in the mid axillary line. Thirteen patients developed disseminated intravascular coagulation (DIC) as diagnosed by five screening tests: prothrombin time (>14 seconds), partial thromboplastin time (>37 seconds), platelet count (<150,000/cu mm), fibrinogen concentration (<0.16 g/dl), and concentration of fibrin degradation products (FDP) (>1:4). The diagnosis was made when in addition to an elevated FDP, three of the other four tests were positive. Bedside balloon occlusion pulmonary angiography was performed in 16 patients.[9] The mean interval between angiography and death was 9.9 ± 7.1 days.

Retrospectively, each patient was allocated to one of three groups according to the interval between intubation and death. In the *early group* (interval less than 9 days—3 days was the earliest in the series) there were five patients with a mean preterminal $\overline{PAP}$ of 35 ± 7.3 mm Hg. The eight patients in the *intermediate group* (10–19 days) had a mean $\overline{PAP}$ of 42.4 ± 9.4 mm Hg, and the 9 patients of the *late group* (20 and more days) had a $\overline{PAP}$ of 42 ± 3.8 mm Hg. The age range, sex distribution, and causes of ARDS were similar in each group. Four patients also had a history of chronic obstructive lung disease, and two had pulmonary carcinoma. There were eight patients with other nonpulmonary diseases, which included cirrhosis (2 patients), carcinoma (2), blood dyscrasia (2), collagen vascular disease (1), and diabetes (1). These were distributed through all duration groups. In all patients, respiratory failure was either the major or a significant contributory cause of death.

Methods

The right lung of 16 patients and left of 6 were obtained at autopsy. In 3 patients only the lower lobe was available for study; in the others, the whole lung. The pulmonary arteries were injected for 4–7 minutes with a barium sulfate gelatin mixture at 60 C and 74 mm Hg pressure. This casting method fills vessels down to about those 15 μ in diameter without filling the capillaries.

The lung was then distended by bronchial instillation of 10% neutral buffered formalin at 30 cm H_2O pressure. After fixation for 1 week, radiographs were taken of the whole lung and then of each of the 1-cm slices into which the specimen was cut. We took arteriograms on Kodak X-Omat TL film, using, for intact lungs, an exposure of 70 kv for 0.8 minutes at 2.25 mÅ and, for the lung slices, 45 kv for 0.3 minutes. The areal density of injected arteries greater than 1 mm in internal lumen diameter (ID) was determined by macroscopic point counting. From each lung 15–25 blocks were selected by stratified random sampling[10] for microscopic sections (2 × 1 cm). Additional sections were taken from any lesion whose type was not included in the random sample.

Tissue was embedded in paraffin, and 4-μ-thick sections were cut and stained with hematoxylin and eosin (H&E) and Miller's elastic van Gieson (EVG) stains. Each slide was examined, and the findings were related to their appearance on the postmortem arteriogram. For detailed morphometric analysis, three or more of the sections from each pulmonary lobe were arbitrarily selected to represent widely separated regions.

With an eyepiece reticle, the external diameter (ED) and medial thickness (MT) of pulmonary arteries were measured across their smallest diameter. External diameter was measured to the external elastic lamina; MT was expressed as 2 MT × 100/ED, where MT is the distance between internal and external elastic laminas. The structure of the pulmonary artery, whether muscular, partially muscular, or nonmuscular, was noted for each vessel, and the structure of the accompanying airway was also recorded. About 25 arteries were measured per slide. We followed the convention of starting from the lower left corner and measuring all filled arteries greater than 20 μ encountered as the slide was scanned from left to right.

Pulmonary artery concentrations were determined by counting all acinar arteries greater than 20 μ in diameter within a given field size (1.65 sq mm). We assessed 10 such fields per slide, using the same slides,

but not necessarily the same fields, as for vascular wall measurements. Areas of lung necrosis or nonfilling were not used for morphometric analysis. The mean concentration of acinar arteries was expressed as arteries per square millimeter. We analyzed the statistical differences in both arterial concentration and wall thickness between the three patient groups using analysis of variance followed by the Newman-Keuls test for multiple comparisons.[11]

Thromboembolic vascular disease was analyzed semiquantitatively. Thrombi in arteries with IDs greater than 1 mm (macrothrombi) were analyzed by direct inspection of all the lung slices. For each lung slice, all clots that occupied more than 10% of the cross-sectional area of arteries with an ID greater than 1 mm were counted. A proportion of these clots were directly sampled for microscopic examination, and the estimate of macrothrombi was determined by multiplication of the number of grossly observed clots by the percentage of thrombi identified histologically. Each lung was scored for macrothrombi from 0 to + + + as follows: 0, no macrothrombi; +, 1-5 macrothrombi; + +, 5-10 macrothrombi; + + +, >10 macrothrombi. Two of the three single lobes obtained for study had more than 10 macrothrombi and were scored as + + +. The other single lobe had between 5 and 10 macrothrombi; and, if one assumed that the upper lobe had a similar concentration of thrombi, the figure was doubled and the patient given a score of + + +. To gauge the extent of thrombosis in arteries with IDs less than 1 mm (microthrombi) for each lung, the percentage of all randomly selected blocks containing at least 1 microthrombus was determined. Lungs were scored from 0 to + + + as follows: 0, no microthrombi; +, thrombi in 0-25% of the slides; + +, thrombi in 25-50% of the slides; + + +, thrombi in >50% of the slides. The angiograms performed antemortem were scored blindly by two radiologists in consultation as having 0, 1, or many pulmonary arterial filling defects.

Finally, tissue for electron-microscopic study was obtained from 6 patients: 4 patients at open lung biopsy, 1 at open biopsy and autopsy, and 1 only at autopsy. Autopsy tissue was obtained within 1 hour of death. The tissue was cut into 1-cu mm fragments, fixed in 2.5% gluteraldehyde for 1-2 hours, washed in 1 M cacodylate buffer, and embedded in Polybed 812 (Polysciences, Warrington, Pa). Sections were cut at 600-800Å, stained *en bloc* with 5% uranyl acetate in buffer and, after sectioning, with 1% uranyl acetate methanol; they were examined with a Philips 300 electron microscope.

Results

General Features

The lungs of patients in the *early group* were heavy, airless, and diffusely dark red-blue. Microscopically they were characterized by interstitial edema, intraalveolar hemorrhage, hyaline membranes, and condensed fibrin in both alveoli and bronchioli. In the *intermediate group* the lungs were more densely consolidated with patchy red-brown and yellow-gray areas. Histologically, there was proliferation of epithelial cells and exuberant organizing granulation tissue. The latter was prominent in alveolar ducts, in some instances obliterating their lumen. Grossly, the lungs of the *late group* were similar to those of the intermediate group but, in addition, contained zones of fine cysts in which air spaces were larger, ranging up to 1 mm in diameter, with walls somewhat thicker than normal. Histologically, mature fibrous tissue was associated with distortion and obliteration of alveolar and bron-

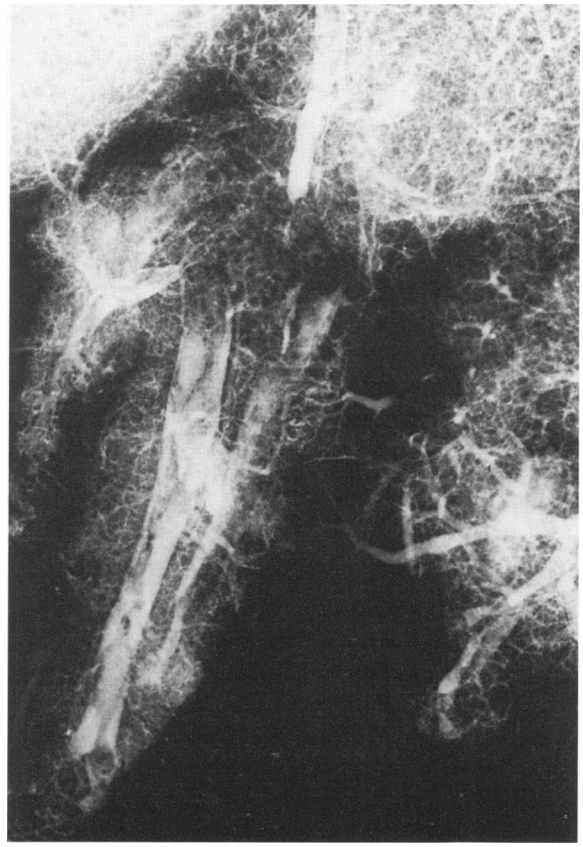

Figure 1 — Postmortem arteriogram showing multiple arterial filling defects due to organizing and recanalized thromboemboli, with reduced filling of peripheral vessels (36 days after aspiration). (×2.6)

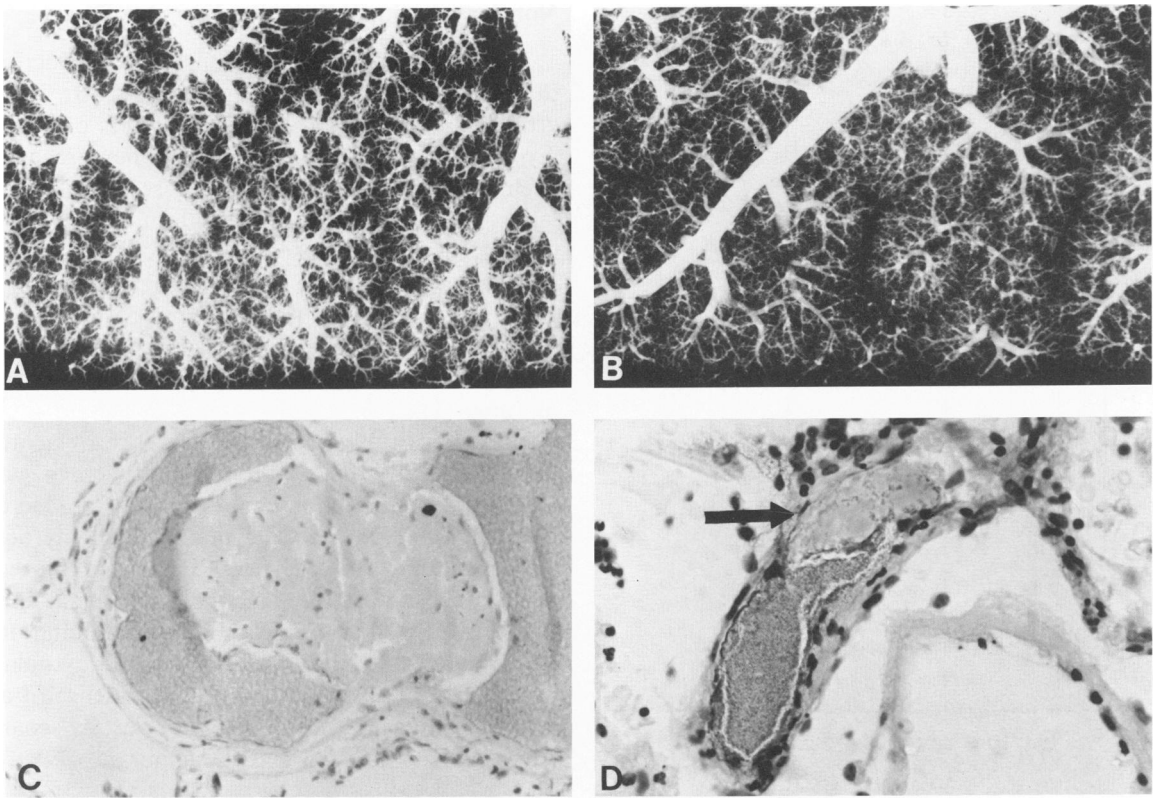

Figure 2—Microthrombosis. **A**—Postmortem arteriogram of normal adult lung. The pleural surface is at the bottom. (×2.4) **B**—Arteriogram of a patient with early ARDS (6 days after aspiration). There are reduced filling of small arteries and prominent, edematous interlobular septa. (×2.4) **C**—Organizing microthrombus adherent to the wall of an alveolar duct artery (17 days after inhalation of toxic fumes). (H&E, ×100) **D**—Platelet fibrin thrombus (*arrow*) obstructing the flow of contrast medium in an alveolar wall artery. A hyaline membrane is below and extravasated red blood cells to the right of the thrombosed vessel (same patient as in **B**). (H&E, ×250) The arteriograms of tissue blocks illustrated in Figures 2, 10, 13, and 14 were taken under the same X-ray exposure.

chiolar spaces. The three patient groups roughly corresponded, respectively, to the exudative, proliferative, and fibrotic stages of diffuse lung injury.[12-14]

Thromboembolic Vascular Disease

Thromboemboli, macroscopically or microscopically identified, were the most consistently observed vascular feature, present in 21 of 22 patients. In the arteriograms, they were present as intravascular filling defects with distal nonfilling. Intravascular linear streaks were due to contrast medium in the recanalized lumens of thrombi (Figure 1).

Macrothrombi were present in 19 patients (86.4%) and were less frequent in those with a prolonged course (Figure 3). Microthrombi, also present in 19 patients (of these, 2 did not have macrothrombi) were of two types (Figure 2). The first type, found in capillaries and small alveolar wall arteries, was a dense, hyaline clot formed of platelets and fibrin. These were numerous in only 3 patients, all in the early group. The second type of microthrombus was found in small preacinar and large intraacinar arteries and often included red and white cells and layered fibrin in addition to hyaline regions. This was the more common type, found in all patient groups as well as in the 3 patients with capillary thrombi (Figure 3). In the postmortem arteriogram, the presence of microthrombi was reflected in reduced filling of small arteries (Figure 2).

The macrothrombus score was highest in patients with multiple pulmonary arterial filling defects on balloon occlusion pulmonary angiography and low in those without these defects (Figure 4). Most patients with filling defects on antemortem angiography had microthrombi, but the number of thrombi varied from patient to patient (Figure 4). The group of 13 patients with a clinical diagnosis of DIC had no distinctive pattern of thrombosis. Eight of these had numerous (+ + − + + +) and five had sparse (+) microthrombi.

In 2 of the 3 patients with numerous capillary

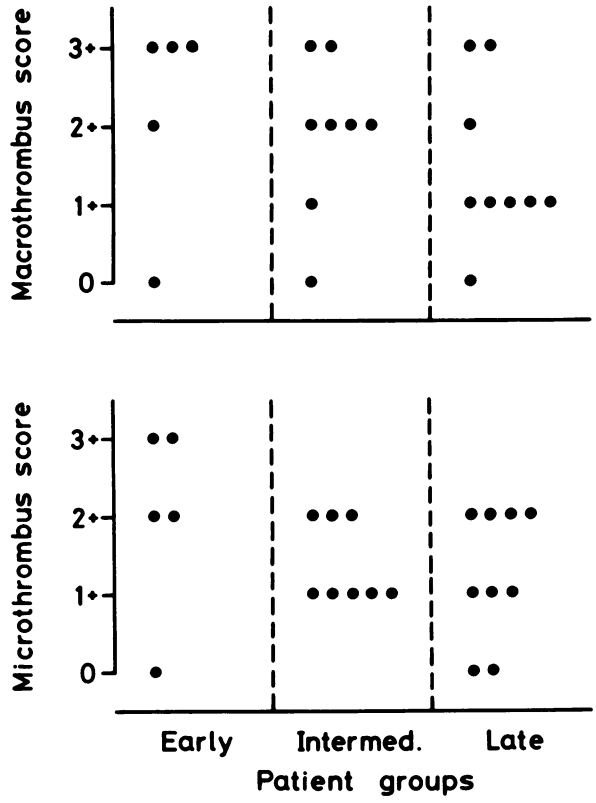

Figure 3—Number of pulmonary thromboemboli found at autopsy related to the duration of ARDS. Lungs were scored semiquantitatively for macrothrombi (*upper*) and microthrombi (*lower*). Each point is the score for a single patient.

platelet fibrin thrombi was the diagnosis of DIC made on the screening tests, but neither of the 2 patients with a microthrombus score of 0 had a positive screen for DIC. Macrothrombi were present in variable numbers in 11 and absent in 2 patients with clinical evidence of DIC.

Infarcts were present in the lungs of 5 patients in the intermediate group and 1 in the late group. Two patients had regions of acellular coagulative necrosis not associated with obstruction of large arteries: in 1 patient from the intermediate group the lung was diffusely necrotic, and in another, from the late group, a 1-cm-deep necrotic band was present subpleurally and posterolaterally. Bone-marrow emboli were prominent in a trauma victim of the early group; whereas refractile, fiber emboli were sparse in 1 late-stage patient. For only 1 patient was an extrapulmonic source of emboli reported at autopsy, although in none of the others was mention made of any special search. In 2 other patients systemic sites of thrombosis had been identified clinically by either venography or radioisotopically labeled fibrinogen.

Nonthrombotic Obliterative Vascular Disease

Postmortem arteriograms showed a reduction in the density of filled small arteries in both the early group and the later groups. In patients of the early group this was due to thrombosis or hemorrhage and edema, which apparently compressed alveolar capillaries. In 7 patients of the intermediate and late groups, necrotizing vasculitis was focal in 5 and in 2 had produced a severe reduction of pulmonary vascular cross-sectional area (Figure 5). In each instance, vasculitis occurred in areas of necrotizing superinfection with bacteria (3 patients), viruses (3), or fungi (1).

Ultrastructurally there was evidence of acute endothelial injury in all the lung specimens we examined. Swollen endothelial cells with rarefied cytoplasm and dilated endoplasmic reticulum encroached upon the lumens of capillaries (Figure 6). Injured endothelial cells were often adjacent to normal-appearing cells. Swollen mitochondria containing membrane-bound vesicles, and occasional cytoplasmic myelin figures provided additional evidence of acute injury. Some endothelial cells were focally separated from the capillary basement membrane (Figure 7),

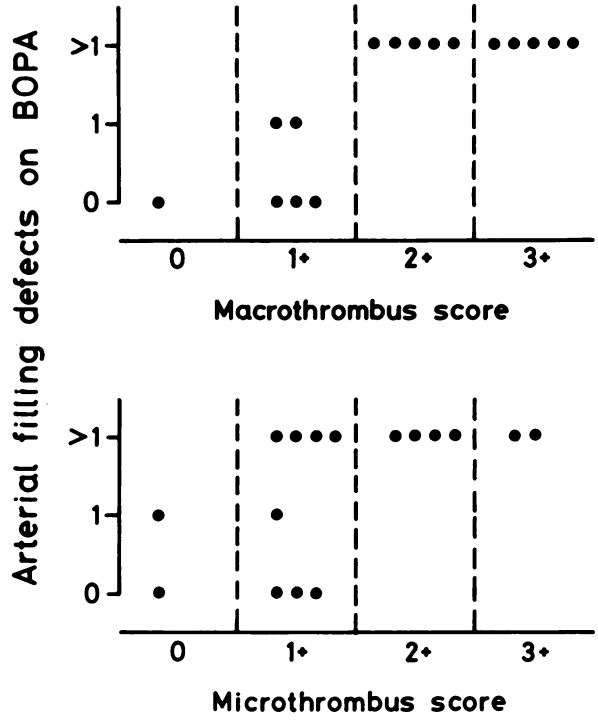

Figure 4—Number of pulmonary thromboemboli found at autopsy related to number of filling defects on antemortem balloon occlusion pulmonary angiograms. Each point represents a single patient.

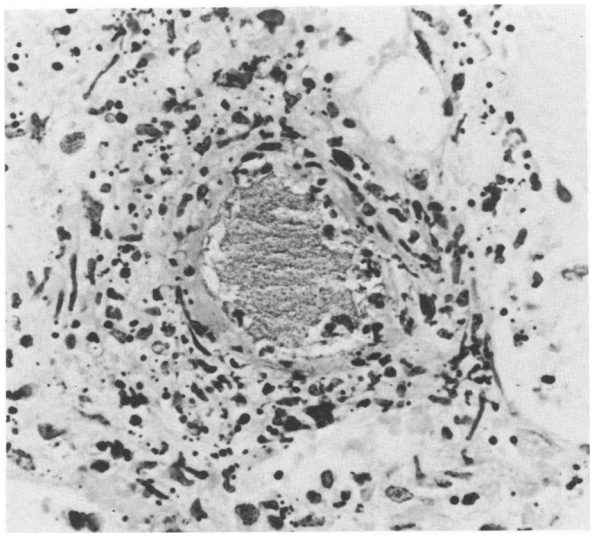

Figure 5—Leukocytoclastic vasculitis with fibrinoid necrosis (16 days, sepsis with secondary herpes pneumonitis). (H&E, ×250).

and in 2 patients necrotic cells had sloughed into the capillary lumen. In nonnecrotic cells, both pinocytotic vesicles and endothelial tight junctions appeared normal. Intraluminally, platelets were infrequently observed, but leukocytes were seen in 3 patients (2 intermediate, 1 late), and obstructed numerous capillaries in the 1 patient whose ARDS followed toxic inhalation. Intracapillary fibrin was noted in 4 patients (2 intermediate, 2 late) and was interposed between sloughed endothelial cells and the basement membrane in 1 from the intermediate group (Figure 7).

In most specimens, capillaries were sparse and difficult to find by electron-microscopic examination. Chronic changes identified ultrastructurally included thickened and reduplicated capillary basement membranes (Figure 8) and hypertrophic endothelial cells with prominent filopodia. In 1 patient in the intermediate group, markedly tortuous capillaries were present against a background of dense, acellular connective tissue (Figure 9). Occasionally, structurally normal pericytes were observed.

In most patients in the intermediate and late groups, many small arteries and intraacinar veins, viewed by light microscopy, were focally obstructed by eccentric or concentric intimal fibrous tissue varying in degree of cellularity (Figure 10). Intimal venous sclerosis was focally distributed and histologically often appeared as sparsely cellular, loose connective tissue arranged in an onionskin pattern (Figure 11). Other veins, particularly in the late group of patients over 40 years of age, had dense hyalinized intimal plaques that stained red with EVG, suggesting collagen. At all stages of the disease, venous thrombi were rare and seen only adjacent to areas of necrosis. Unfortunately, these larger arteries and veins were not represented in the tissue studied electron-microscopically.

The pulmonary lymphatics also showed structural alterations. In all patients, dilated lymphatic channels were prominent. Additionally, in 10 patients, 5 each from the intermediate and late groups, there was focal narrowing of the lumens of interlobular and subpleural lymphatics by sparsely cellular loose connective tissue (Figure 12).

Chronic Vascular Remodeling

In patients in the late group extensive remodeling of the pulmonary vascular bed had occurred. The arteriogram showed narrow preacinar arteries stretched and splayed about fibrous-walled cysts and dilated air spaces. Beneath the pleura these stretched vessels focally had a "picket fence" appearance (Figure 10). In all late group patients tortuous preacinar and intraacinar arteries were present in the arteriogram and appeared histologically as serpentine, kinked and coiled, thick-walled vessels (Figure 13). These tortuous channels were concentrated in regions of dense or irregular fibrosis. An associated histologic finding in the late-stage patients was irregularly distributed nests of dilated capillaries that abnormally admitted contrast medium into the pulmonary veins. In 7 patients this produced a dense, ground-glass background haze in the postmortem arteriogram (Figure 14).

Morphometric Findings

Figure 15 shows the arterial concentrations for the 3 patient groups. Compared to the early group, the intermediate group had a reduced, and the late stage patients an increased, mean concentration of intraacinar arteries. In neither did this reach statistical significance, because the variance between patients, especially in the late groups, was great.

With increasing duration of ARDS there was a steady reduction in mean external diameter for partially and fully muscular arteries (Figure 16). For the fully muscular arteries this difference was significant between the early and late groups, and for the partially muscular arteries both the early and intermediate groups were significantly different from the late group.

As the duration of ARDS increases, the percentage

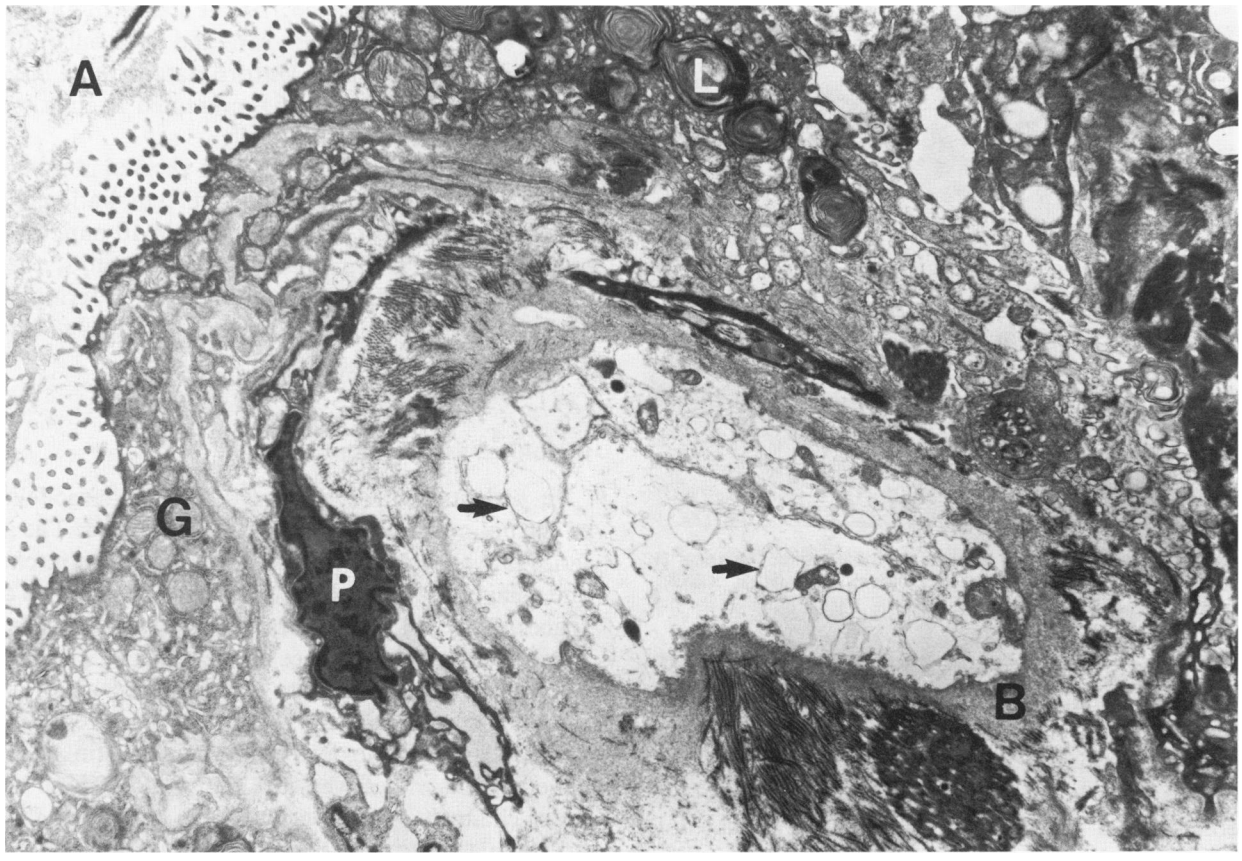

Figure 6 – Acute endothelial injury. Swollen endothelial cells with dilated endoplasmic reticulum (*arrows*) occlude the capillary lumen. A pericyte (*P*) is adjacent to the thickened basement membrane (*B*). Granular pneumonocytes (*G*) with prominent microvilli and lamellar inclusions (*L*) line the alveolus (*A*) (16 days, viral pneomonia). (×6500)

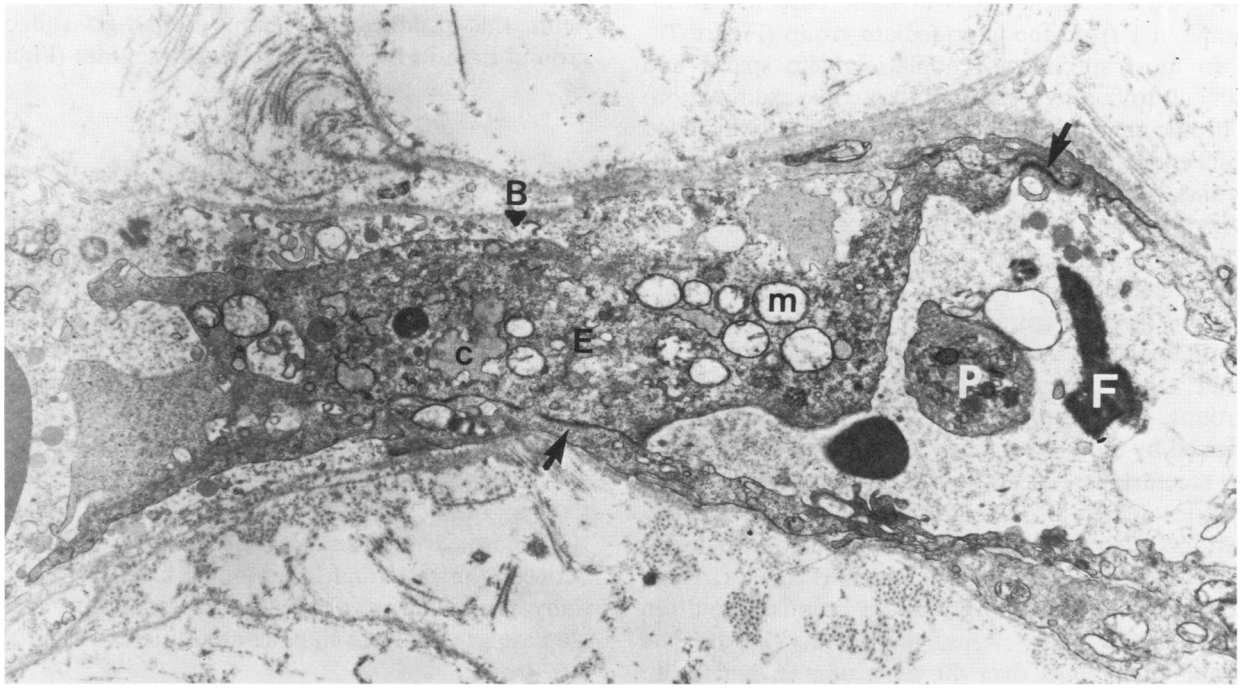

Figure 7 – Acute endothelial injury. Early separation of endothelial cell (*E*) from capillary basement membrane (*B*) with interposition of fibrin and cellular debris. Mitochondria (*M*) and cisternae (*C*) are swollen, but intercellular junctions are still intact (*arrows*). Platelets (*P*), fibrin (*F*), and membrane-bound debris lie within capillary lumen on right (biopsy, Day 10, toxic inhalation). (×6580)

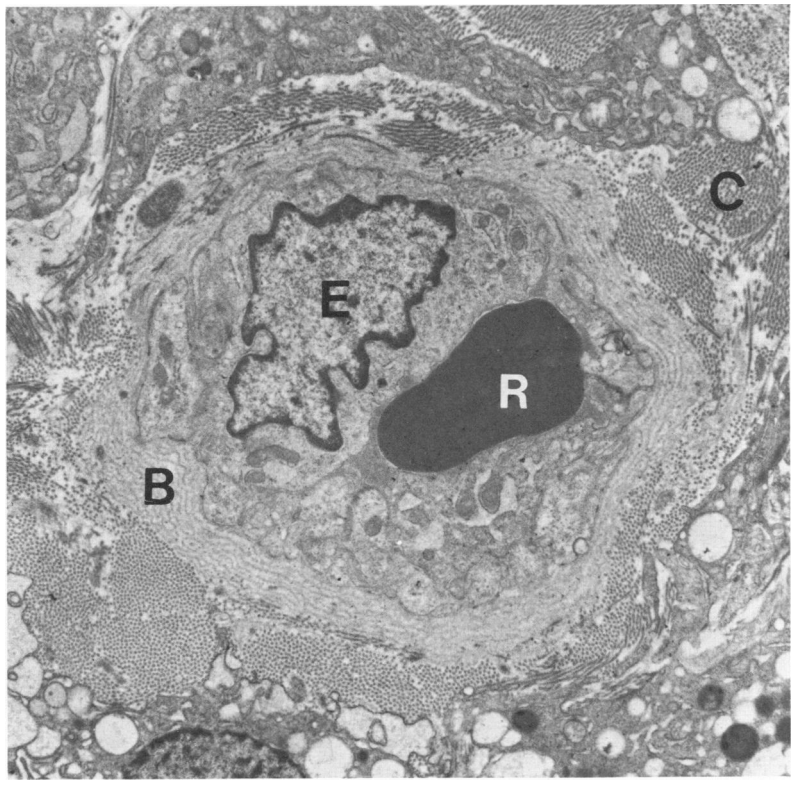

Figure 8—Chronic injury. A prominent endothelial cell (*E*) narrows the capillary lumen that is filled by a distorted red blood cell (*R*). The basement membrane (*B*) is reduplicated, and there is abundant perivascular collagen (*C*) (25 days after aspiration). (×6580)

of medial wall thickness increases (Figure 17). If both acinar and preacinar muscular arteries are combined, this change is significantly different between the early and late groups. The trend toward increasing wall thickness, however, was present at each landmarked level of the pulmonary artery (Figure 18). Changes in wall thickness between patients of the early and intermediate groups were most notable at the preacinar level, whereas differences in both preacinar and intraacinar arteries were significant between the early and late groups.

When one compares individual patients, the variance in the percentage of medial thickness increases with duration of ARDS (Figure 19). In the patients of the early group there is a narrow distribution of thin-walled arteries. With increasing duration of lung injury, the range becomes wider and shifts toward greater medial wall thickness.

Discussion

The term "adult respiratory distress syndrome" designates a clinical illness characterized by acute, catastrophic respiratory failure with hypoxemia, decreased pulmonary compliance, increased microvascular permeability, and diffuse alveolar infiltrates on chest X-ray. Though intrapulmonary processes may produce this syndrome, it is most puzzling when, as often happens, it is precipitated by a nonpulmonary illness such as systemic trauma or sepsis. Despite the diversity of causes, the pathologic picture is fairly constant, usually with few hints of the original cause.[15] Pathologically the syndrome can be divided into an early, "exudative" phase, which evolves, after about a week, into a "proliferative" phase.[12-14] In the present study we have divided the patients according to duration of ARDS, from the onset of severe disease (tracheal intubation) into early, intermediate, and late groups, which correspond with three key stages in the pathologic evolution of the disease—the acute exudative phase of edema and hemorrhage, the stage of exuberant granulation tissue associated with organization of fibrinous edema, and the stage where this edema is converted to dense fibrosis. The development of pulmonary vascular lesions in ARDS relates to this time frame. For any patient, the pulmonary vascular lesions correlate with the duration of pulmonary disease rather than its cause.

Whereas simple loss of the pulmonary vascular bed in this syndrome has been previously described,[1,8] the wide variety of vascular lesions is herein identified. When related to the progression of disease, new types of vascular lesions appear even in the intermediate and late phases. While some lesions may represent

Figure 9—Distorted tortuous pulmonary capillary. *E*, endothelial cell; *R*, red blood cell (biopsy, 16 days after trauma). (×6580)

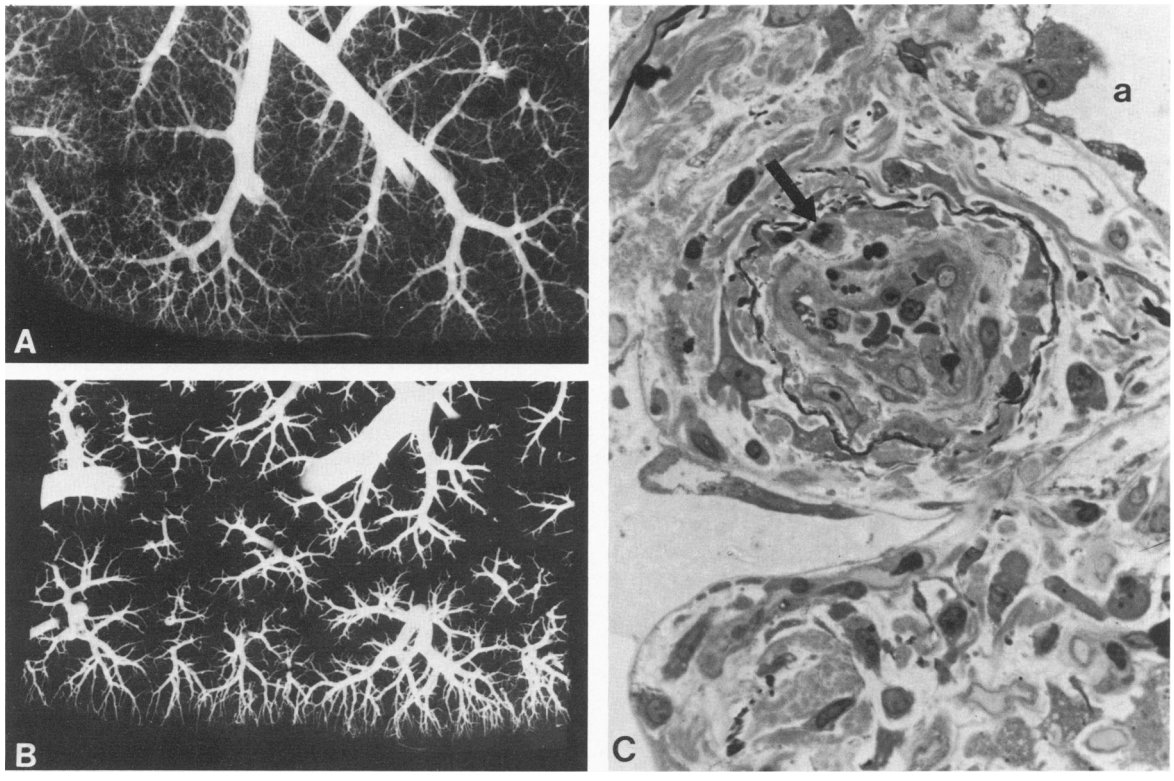

Figure 10—Fibrocellular vascular obliteration. **A**—Postmortem arteriogram showing marked reduction of filled small vessels and prominent interlobular septa (16 days, viral pneumonitis). (×2.4) **B**—More extensive reduction of filled peripheral arteries due to intimal obliteration. Subpleural branches are stretched about dilated air spaces with a "picket fence" appearance (16 days after toxic inhalation). (×2.4) **C**—Severe fibrocellular intimal proliferation in a nonmuscular alveolar wall artery. Note cell in mitosis (*arrow*). The interstitium is widened by collagen, edema, and a mononuclear cell infiltrate. Irregular hyperplastic epithelial cells line alveolar spaces (*a*) (biopsy, Day 21, viral pneumonia). (Toluidine blue, ×400)

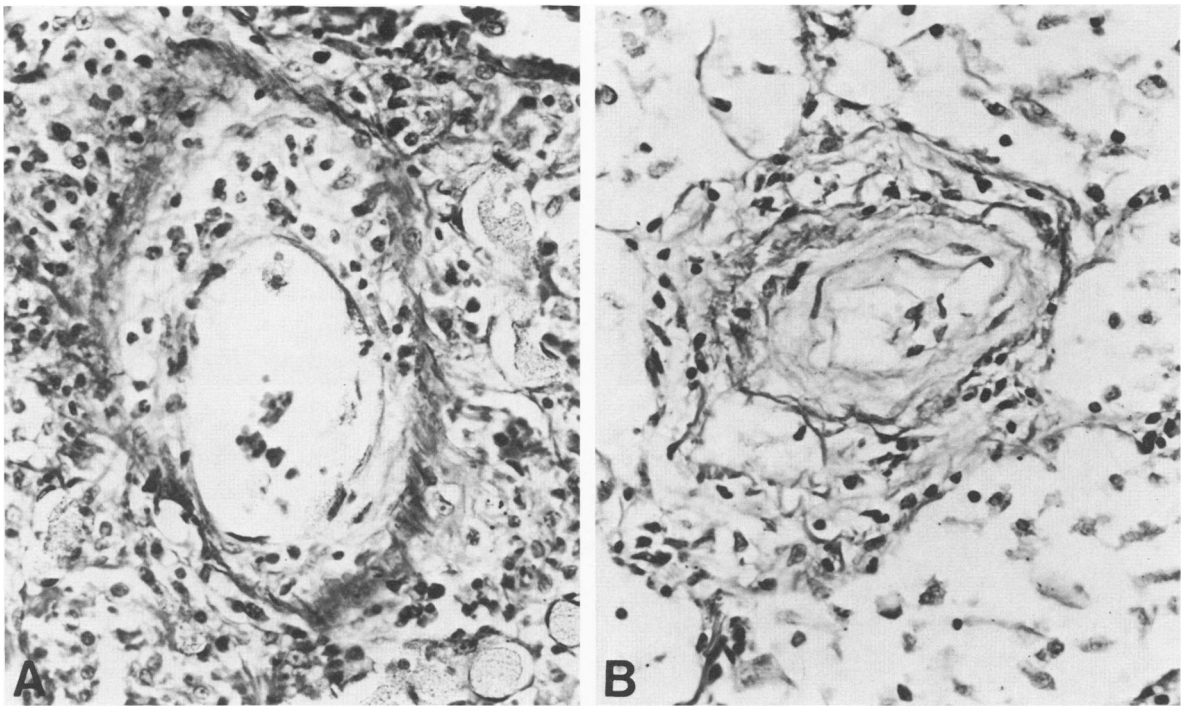

Figure 11 — Venous sclerosis. **A** — Eccentric fibrous intimal thickening of a pulmonary vein with cellular intra- and perivascular infiltrate of fibroblasts, lymphocytes, plasma cells, and a few neutrophils (36 days after aspiration). (Elastic van Gieson, ×250) **B** — Lumen of an intralobular vein narrowed by loose connective tissue (20 days after trauma). (Elastic van Gieson, ×250)

the evolution of antecedent injury, others, such as late-onset acute endothelial injury are probably the result of superimposed events such as high FI_{O_2} or superinfection.

All of these vascular lesions can contribute to pulmonary hypertension. In the early stage, acute endothelial injury has been documented ultrastructurally within 1 day of the onset of symptoms.[16] At the light-microscopic level, intense hemorrhage and edema is associated with intracapillary engorgement and microvascular thromboemboli. These changes persist into the intermediate phase when chronic capillary changes are observed ultrastructurally. This phase is further characterized by fibrocellular obliteration of arteries, veins, and even lymphatics. Often during the intermediate phase, severe pulmonary infection supervenes and produces necrotizing vasculitis. Finally, in the late stage, vascular remodeling is associated with distorted, tortuous arteries and veins and a reduced number of capillaries, which are typically dilated. Arterial muscularization and neomuscularization is identified morphometrically in the intermediate phase and is pronounced in the late phase.

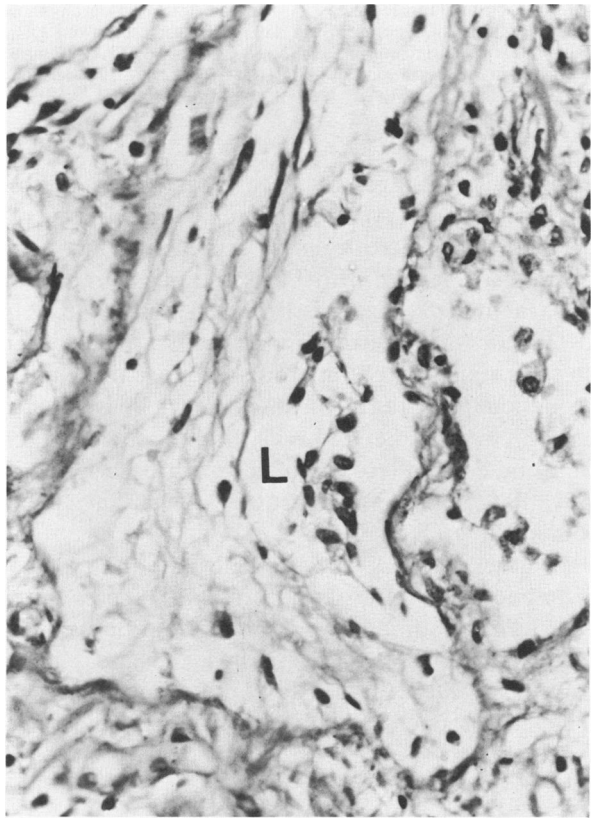

Figure 12 — Lymphatic duct lumen (*L*) narrowed by loosely organized, sparsely cellular connective tissue. The surrounding interlobular septum is fibrotic (20 days after trauma). (Elastic van Gieson, ×250)

Thromboembolism

The quantitative methods used in this study demonstrate the importance of thromboemboli

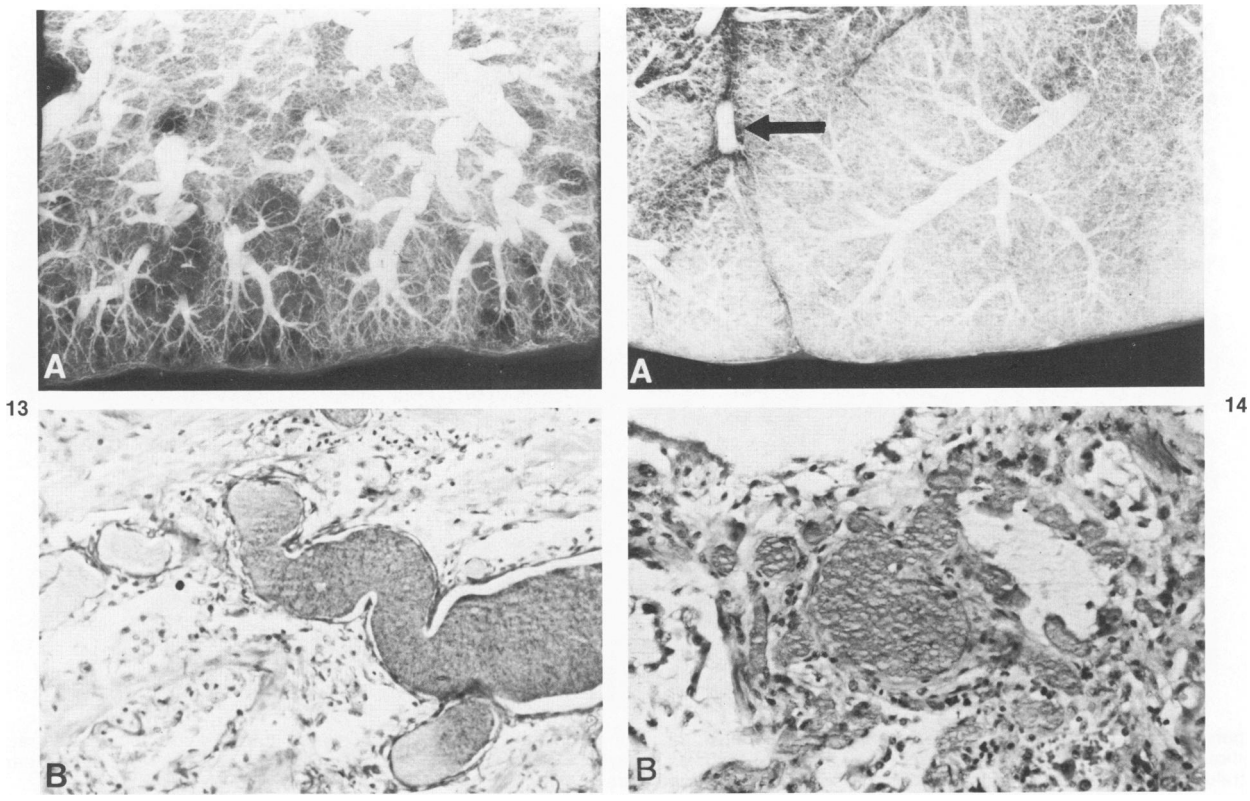

Figure 13—Arterial tortuosity. **A**—Postmortem arteriogram showing marked arterial tortuosity, increased background haze, and fine arteries stretched about honeycomb "cysts" (26 days after aspiration). (×2.4) **B**—Serpentine acinar arteries are surrounded by organizing fibrous tissue (same patient as in **A**). (Elastic van Gieson, ×100) **Figure 14**—Capillary dilatation. **A**—Postmortem arteriogram showing intense background haze and venous filling (*arrow*) (55 days after viral pneumonia). (×2.4) **B**—Nests of dilated capillaries, filled with barium and surrounded by fibrous tissue (same patient as **A**). (H&E, ×250)

throughout all stages of disease of diverse causes. The morphologic types of thromboemboli—macrothrombi, large microthrombi, and capillary thrombi—have been described by Eeles and Sevitt in burned and traumatized patients.[17] As in that study, in ARDS, capillary microthrombi are most numerous in the early stage. Larger microthrombi occur regularly throughout all stages of disease, whereas macrothrombi tend to be fewer in the late stage, which could indicate either lysis of macrothrombi or, perhaps, that the patients that survive longer have fewer clots in the early stages.

We attempted to correlate the extent and types of thromboemboli found at autopsy with the cause of the ARDS, the findings on antemortem balloon occlusion pulmonary angiography, and the clinical diagnosis of DIC. In our study there was no pattern of macro or microthrombosis characteristic of any single cause of ARDS. The lung scores for macrothrombi correlated with filling defects noted on balloon occlusion pulmonary angiography; scores for microthrombi did not correlate as well. Greene et al have previously reported filling defects in 48% of patients with ARDS and shown that the presence of multiple filling defects is an early indicator of eventual death.[9]

The clinical diagnosis of DIC by standard screening tests did not reliably predict thromboemboli at autopsy. Although a clinical diagnosis of DIC was

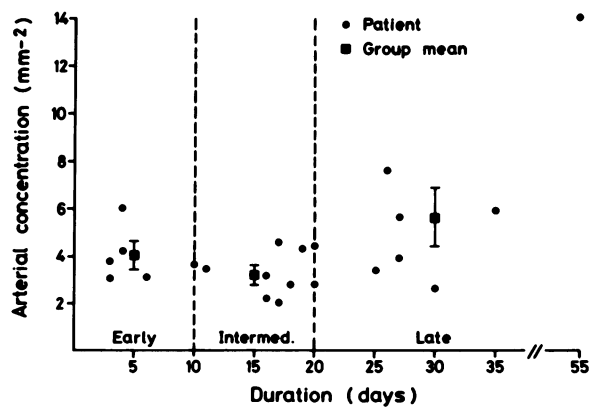

Figure 15—Concentration of intraacinar arteries related to the duration of ARDS. *Circles* represent individual patients; *squares* represent group means ± SEM.

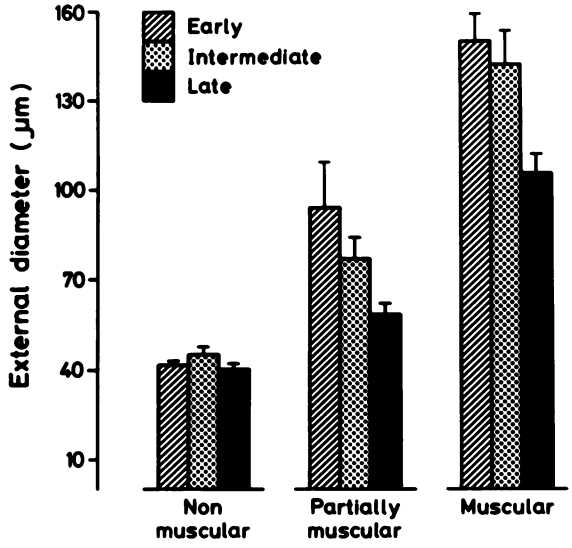

Figure 16—Variation in the external diameter of three structural types of intraacinar arteries with duration of ARDS (mean ± SEM). For partially muscular arteries, both early and intermediate groups are significantly different from the late group ($P < 0.05$). For muscular arteries the early group differs significantly only from the late group ($P < 0.01$).

associated with at least some thromboemboli, that diagnosis did not necessarily indicate large numbers of thromboemboli. There were also 6 patients in whom the diagnosis of DIC could not be made by laboratory screening tests but who also had thromboemboli at autopsy. If more sensitive coagulation tests are used, most patients with ARDS show evidence of intravascular clotting.[18] In retrospective studies such as this, however, the timing of the coagulation blood sample as well as the interval between this sample and death will obviously affect the correlations.

The origin and pathogenicity of thromboemboli in ARDS is controversial. Eeles and Sevitt believed that, in burn and trauma patients, both macrothrombi and microthrombi originated as systemic venous thrombi. They believed capillary thrombi were related to hypercoagulation immediately after severe injury. In their study this view was supported by the finding of deep vein thrombosis in the extremities of most patients with pulmonary thromboemboli.[17] Others have also demonstrated that, particularly after shock or trauma, microemboli may originate peripherally.[3,4,19] On the other hand, pulmonary endothelial injury in ARDS can cause localized intravascular coagulation within the lung.[20,21] Furthermore, Boggis et al have documented *in situ* microthrombosis after experimental lung contusion in sheep.[22] The present study cannot resolve the problem of the origin of pulmonary thromboemboli in ARDS, because it is impossible on morphologic grounds to distinguish embolic clots from those developing *in situ*.

Microemboli have been assigned a primary pathogenetic role in producing lung injury, especially in ARDS following trauma and shock.[3,4,23,24] We could not reach a firm conclusion about the role of microemboli as mediators of primary lung injury in all instances of ARDS. The absence of thromboemboli in some patients, including 1 early group patient with findings typical of the exudative phase, and the presence of severe lung injury in a patient with aplastic anemia suggest that microemboli are not the only mediators of acute lung injury in this disease. Only 3 patients in our series had numerous capillary thrombi, the form most likely to produce diffuse lung injury. The possibility, however, that capillary microthrombi were present and subsequently lysed in patients with longer survival cannot be excluded. Whether or not they represent a primary triggering mechanism, thromboemboli can contribute to lung injury at any stage, further reducing the pulmonary vascular bed and producing lung necrosis through ischemia.

Endothelial Injury

While acute endothelial injury has been reported as an early event in ARDS, an important finding in this study was the presence of acute changes even in the intermediate and late stages. The cellular changes

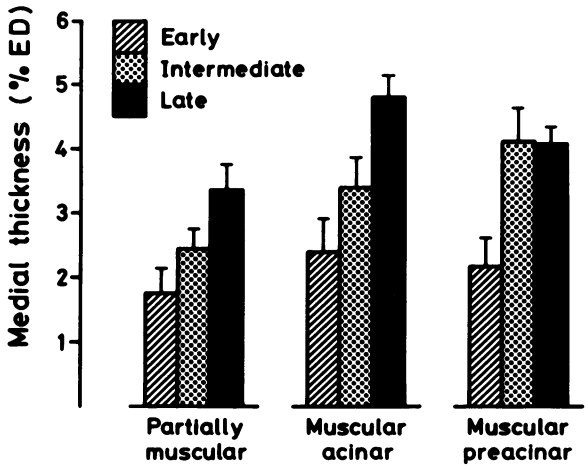

Figure 17—Variation in the percentage of medial wall thickness of partially and fully muscular arteries with duration of ARDS (mean ± SEM). For partially muscular arteries the early group differs significantly from the late group ($P < 0.05$). For muscular acinar arteries both the early ($P < 0.01$) and intermediate groups ($P < 0.05$) differ significantly from the late group, whereas for preacinar arteries, the early group differs from both the intermediate group ($P < 0.05$) and the late group ($P < 0.01$).

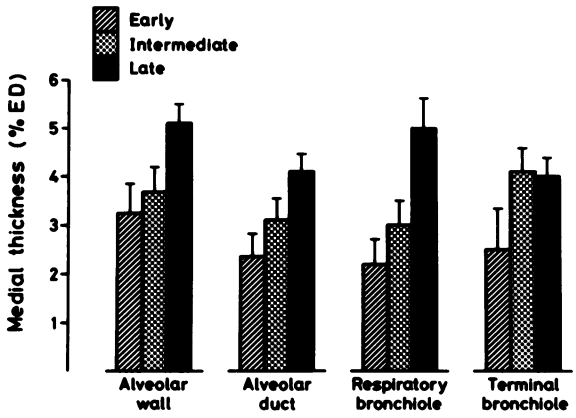

Figure 18—Variation in the percentage of medial wall thickness of muscularized pulmonary arteries at different anatomic levels with duration of ARDS. The early group differs significantly from the late group at the alveolar duct ($P < 0.05$) and respiratory bronchiolar levels ($P < 0.01$). There is significant difference between the intermediate and late groups only at the respiratory bronchiolar level ($P < 0.05$).

were similar regardless of the cause of ARDS and resemble those reported in ARDS due to sepsis, shock, or thermal injury.[8,16,25] Similar capillary endothelial changes occur in humans and animals exposed to toxic levels of oxygen[26-29] and in many different experimental models of acute lung injury.[30-35] The presence of acute changes long after the initial injury suggests additional noxious factors, such as a high FI_{O_2}, may produce additive injuries in later stages of the disease. In the intermediate and late groups chronic changes such as hypertrophic endothelial cells and thickened, reduplicated basement membranes compromise capillary lumens.

Fibrous Intimal Proliferative Lesions

Throughout the intermediate and late stages there was reduced filling of small arteries in the postmortem arteriogram. Fibrocellular intimal proliferation of arteries contributes to the reduction in cross-sectional luminal area and is a nonspecific finding that can be associated with severe pulmonary hypertension of various types, interstitial fibrosis, or pulmonary inflammation.[36] A similar intimal change, associated with reduced angiographic filling, has been described in the experimental animal breathing oxygen for 28 days.[37]

In ARDS a similar, but generally less cellular intimal proliferation occurs focally in pulmonary veins. Physiologically, venous obstruction can contribute to elevated microvascular pressure and force fluid into the extravascular space. Obstruction of lymphatics secondary to coagulation of proteinaceous edema will further impede removal of interstitial fluid. The endolymphatic obstruction observed in this study, involving relatively large interlobular channels, suggests a more widespread functional obstruction of small intralobular lymphatics.

Chronic Vascular Remodeling

Extensive pulmonary vascular remodeling occurs in the intermediate and chronic phases of ARDS. Preacinar arteries, stretched and distorted by surrounding parenchymal fibrosis, create unusual arteriographic patterns. Arterial tortuosity is often extensive. It appears to be a nonspecific vascular distortion by forces exerted via irregular, contracting fibrous tissue, an "accordion effect." Changes of vascular wall compliance by chronic injury could also, in part, contribute to this appearance. In patients in the late stage, pulmonary capillaries are markedly dilated, forming irregular cirsoid nests. The increased arterial concentrations we measured in patients in the late stage probably reflects the abnormally dilated vessels, and not a restoration or regrowth of normal arteries.

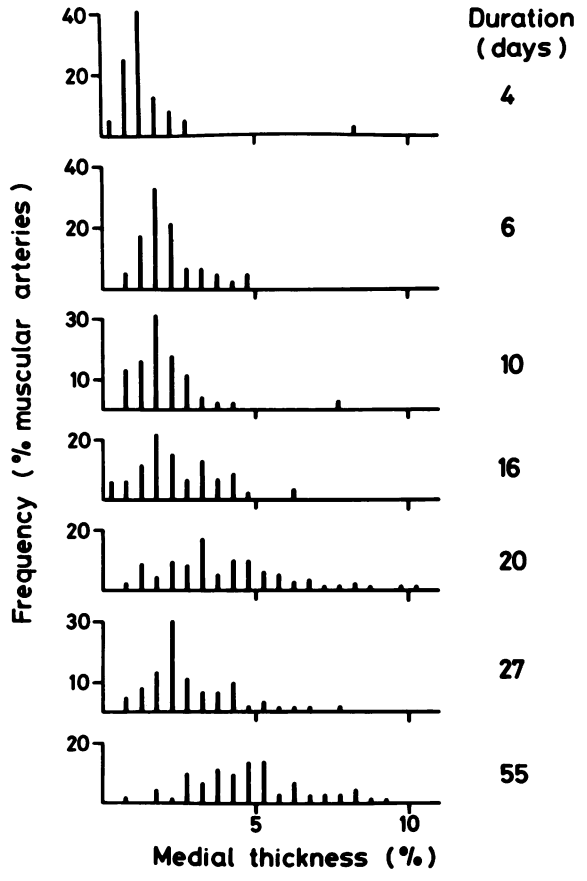

Figure 19—Frequency distribution of the percentage of medial wall thickness of muscular pulmonary arteries for individual lungs, arranged according to increasing duration of ARDS. Representative patients have been selected to show the trend of changes.

Muscularization and Neomuscularization

The present morphometric findings extend those of Snow et al.[7] and show for the first time a significant increase in arterial muscularity with time during ARDS. The decreased mean external diameter of fully and partially muscular arteries in patients in the intermediate and late stages suggests that smaller partially muscular or nonmuscular arteries have been "recruited" into the muscular group by peripheral extension of muscle into smaller arteries than is normal. The presence of a significant difference in medial wall thickness between the early and intermediate groups only at the preacinar level suggests further that muscularization starts centrally.

There are several possible mechanisms contributing to increased arterial muscularization in ARDS. Hypoxia, which is present early and may be either diffuse or localized within the lung in ARDS, causes muscular hypertrophy and extension in man and experimental animals.[38-40] Pulmonary hypertension itself may lead to both types of muscularization, as seen in patients with congenital heart disease and high-flow left-to-right shunts.[41] In the irregularly reduced vascular bed of ARDS there may be localized increased flow. Finally, oxygen toxicity may play a key role in both the acute and more chronic vascular lesions. In chronic experimental hyperoxia arterial muscularization and muscular extension has been observed.[37] The net effect of increased mural musculature will be to further reduce the vascular lumen diameter and possibly increase vascular tone and reactivity.

Clinical Implications

The vascular lesions of ARDS correlate more with the duration of disease than with the particular cause. They vary in their nature and severity, are largely nonspecific, and do not identify any specific mechanism of injury, but are compatible with the sequelae of different types of vascular insult. The findings in this study, however, have important therapeutic implications. Diagnosis and treatment of thromboembolic disease with anticoagulant or thrombolytic therapy could preserve segments of the pulmonary artery. Similarly, treatment of infectious complications by appropriate antibiotics should reduce vasculitis. Minimizing exposure to high levels of oxygen, a potent endothelial toxin, should also limit vascular injury. An understanding of the basic mechanisms of lung injury in ARDS may eventually lead to the development of specific pharmacologic agents to protect the vascular endothelium from the noxious effects of mediators such as superoxide radicals, vasoactive peptides, and metabolites of arachidonic acid.[42] Finally, early intervention in ARDS is essential, because many of the chronic vascular changes such as capillary or lymphatic obliteration and vascular tortuosity appear to be irreversible, contribute to progressive lung destruction, and prevent survival.

References

1. Zapol WM, Snider MT: Pulmonary hypertension in severe acute respiratory failure. N Engl J Med 1977, 296:476-480
2. Pontoppidan H, Wilson RS, Rie MA, Schneider RC: Respiratory intensive care. Anesthesiology 1977, 47:96-116
3. Blaisdell FW, Lim RC, Stallone RJ: The mechanism of pulmonary damage following traumatic shock. Surg Gynecol Obstet 1970, 130:15-22
4. Saldeen T: The microembolism syndrome. Microvasc Res 1976, 11:227-259
5. West JB, Dollery CT, Heard BE: Increased pulmonary vascular resistance in the dependent zone of the isolated dog lung caused by perivascular edema. Circ Res 1965, 17:191-206
6. Zapol WM, Kobayashi K, Snider MT, Greene R, Laver MB: Vascular obstruction causes pulmonary hypertension in severe acute respiratory failure. Chest 1977, 71S(suppl):306-307
7. Snow RL, Davies P, Pontoppidan H, Zapol WM, Reid LM: Pulmonary vascular remodelling in adult respiratory distress syndrome. Am Rev Respir Dis 1982, 126:887-892
8. Bachofen M, Weibel ER: Alterations in gas exchange apparatus in adult respiratory insufficiency associated with septicemia. Am Rev Respir Dis 1977, 116:589-615
9. Greene R, Zapol WM, Snider MT, Reid L, Snow R, O'Connell RS, Novelline RA: Early bedside detection of pulmonary vascular occlusion during acute respiratory failure. Am Rev Respir Dis 1981, 124:593-601
10. Dunnill MS: Quantitative methods in the study of pulmonary pathology. Thorax 1962, 17:320-328
11. Snedecor GW, Cochran WG: Statistical Methods. 6th edition. Ames, Iowa, The Iowa State University Press, 1967, p 273
12. Katzenstein AL, Bloor C, Liebow AA: Diffuse alveolar damage, the role of oxygen, shock and related factors. Am J Pathol 1976, 85:210-228
13. Orell SR: Lung pathology in respiratory distress following shock in the adult. Acta Pathol Microbiol Scand 1971, 79:65-76
14. Nash G, Blennerhassett JB, Pontoppidan H: Pulmonary lesions associated with oxygen therapy and artificial ventilation. N Engl J Med 1967, 276:368-374
15. Pratt PC, Vollmer RT, Shelburne JD, Crapo JD: Pulmonary morphology in a multihospital collaborative extracorporeal membrane oxygenation project: I. Light microscopy, Am J Pathol 1979, 95:191-208
16. Schnells G, Voigt WH, Redl H, Schlag G, Glatzl A: Electron microscopic investigation of lung biopsies in patients with post traumatic respiratory insufficiency. Acta Chir Scand (S) 1980, 449:9-20
17. Eeles GH, Sevitt S: Microthrombosis in injured and burned patients. J Pathol Bacteriol 1967, 93:275-293
18. Carvalho A, Greene R, Boggis C, Quinn D, Rie M, Zapol W: Intravascular coagulation (IVC) with fibrinolysis in patients with acute respiratory failure (ARF)

and angiographic pulmonary vascular occlusion (Abstr). Am Rev Respir Dis 1982, 125(suppl):93
19. Blaisdell FW, Lim RC, Amberg JR, Choy SH, Hall AD, Thomas AN: Pulmonary microembolism, a cause of morbidity and death after major vascular surgery. Arch Surg 1966, 93:776–786
20. Bone RC, Francis PB, Pierce AK: Intravascular coagulation associated with the adult respiratory distress syndrome. Am J Med 1976, 61:585–589
21. Schneider RC, Zapol WM, Carvalho AC: Platelet consumption and sequestration in severe acute respiratory failure. Am Rev Respir Dis 1980, 122:445–451
22. Boggis C, Greene R, Schuette A, Tomashefski J, Jones R: Pulmonary arterial occlusive disease in experimental lung contusion (Abstr). Invest Radiol 1982, 17:58
23. Lough J, Moore S: Endothelial injury induced by thrombin or thrombi. Lab Invest 1975, 33:130–135
24. Costabella PM, Lindquist O, Kapanci Y, Saldeen T: Increased vascular permeability in the delayed microembolism syndrome, experimental and human findings. Microvasc Res 1978, 15:275–286
25. Nash G, Foley FD, Langlinais PC: Pulmonary interstitial edema and hyaline membranes in adult burn patients, electron microscopic observations. Hum Pathol 1974, 5:149–159
26. Gould VE, Tosco R, Wheelis RF, Gould NS, Kapanci Y: Oxygen pneumonitis in man, ultrastructural observations on the development of the alveolar lesions. Lab Invest 1972, 26:499–508
27. Kapanci Y, Weibel ER, Kaplan HP, Robinson FR: Pathogenesis and reversibility of the pulmonary lesions of oxygen toxicity in monkeys: II. Ultrastructural and morphometric studies. Lab Invest 1969, 20:101–116
28. Kistler GS, Caldwell PRB, Weibel ER: Development of fine structural damage to alveolar and capillary lining cells in oxygen poisoned rat lungs. J Cell Biol 1967, 32:605–628
29. Crapo JD, Peters-Golden M, Marsh-Salin J, Shelburne JS: Pathologic changes in the lungs of oxygen adapted rats, a morphometric analysis. Lab Invest 1978, 39:640–653
30. Connell RS, Swank RC, Webb MC: The development of pulmonary ultrastructural lesions during hemorrhagic shock. J Trauma 1975, 15:116–129
31. Connell RS, Swank RL: Pulmonary microembolism after blood transfusions, an electron microscopic study. Ann Surg 1977, 177:40–50
32. Ratliff NB, Wilson JW, Hackel DB, Martin A: The lung in hemorrhagic shock: II. Observations on alveolar and vascular ultrastructure. Am J Pathol 1970, 58:353–373
33. Fishman AP: Electron microscopic alterations at the alveolar level in pulmonary edema. Circ Res 1967, 21:783–797
34. Boatman ES, Frank R: Morphologic and ultrastructural changes in the lungs of animals during acute exposure to ozone. Chest 1974, 65(suppl):9–11
35. Alexander IGS: The ultrastructure of the pulmonary alveolar vessels on Mendelson's (acid pulmonary aspiration) syndrome. Br J Anaesthesiol 1968, 40:408–414
36. Wagenvoort CA, Wagenvoort N: Pathology of pulmonary hypertension. New York, John Wiley & Sons, 1977, pp 273–282
37. Jones R, Zapol WM, Reid L: Progressive and regressive structural changes in rat pulmonary arteries during recovery from prolonged hyperoxia (Abstr). Am Rev Respir Dis 1982, 125(suppl):227
38. Naeye RL: Hypoxemia and pulmonary hypertension. Arch Pathol Lab Med 1961, 71:447–452
39. Hislop A, Reid L: New findings in pulmonary arteries of rats with hypoxia-induced pulmonary hypertension. Br J Exp Pathol 1976, 57:542–553
40. Meyrick B, Reid L: The effect of continued hypoxia on rat pulmonary artery circulation: An ultrastructural study. Lab Invest 1978, 38:188–200
41. Hislop A, Haworth SG, Shinebourne EA, Reid L: Quantitative structural analysis of pulmonary vessels in isolated ventricular septal defect in infancy. Br Heart J 1975, 37:1014–1021
42. Hempel FG, Lenfant CJM: Current and future research on adult respiratory distress syndrome. Semin Respir Med 1981, 11:165–172

Acknowledgments

The authors thank Dr. Antonio Perez, who reviewed the electron micrographs, and Peter Nowak, who prepared them, Tudor Williams and Marita Bitans for photographic assistance, and Pamela Conze and Priscilla Stottlemire for secretarial help. The authors are also deeply appreciative of the cooperation of Drs. Robert McCluskey and Eugene Mark of the Department of Pathology, Massachusetts General Hospital.